Paper No. T1-2.3, pp. 1-6

15th INTERNATIONAL SYMPOSIUM on
POWER ELECTRONICS - Ee 2009
XV Međunarodni simpozijum Energetska elektronika – Ee 2009
NOVI SAD, REPUBLIC OF SERBIA, October 28th - 30th, 2009

EXPERIMENTAL VERIFICATION OF SINUSOIDAL APPROXIMATION IN ANALYSIS OF THREE-PHASE TWELVE-PULSE OUTPUT VOLTAGE TYPE RECTIFIERS

Predrag Pejović[1], Johann W. Kolar[2], Vladimir Šviković[1]
[1]Faculty of Electrical Engineering, University of Belgrade, Belgrade, Serbia
[2]Swiss Federal Institute of Technology, Zürich, Switzerland

Abstract: *Experimental verification of the sinusoidal approximation approach in analysis of three-phase twelve-pulse output voltage type rectifiers is presented in the paper. The rectifier operating parameters: dependence of the output voltage on the output current, the output power, the power factor, and the efficiency, are determined applying sinusoidal approximation. The analytical predictions are verified on a low-power experimental rectifier model.*

Keywords: ***AC-DC power conversion, converters, harmonic distortion, power conversion harmonics, power quality, rectifiers.***

1. INTRODUCTION

In this paper, suitability of the sinusoidal approximation approach in modeling of the rectifier presented in Fig. 1 is analyzed. The rectifier of Fig. 1 is proposed in [1], and it consists of three coupling inductors, a line-side interphase transformer, two diode bridges, and a filtering capacitor. The line-side interphase transformer splits the input currents and provides equal load sharing between the diode bridges. Besides, it provides appropriate phase shift to form twelve-pulse voltages v_{T1}, v_{T2}, and v_{T3} on the basis of v_{A1}, v_{A2}, v_{A3}, v_{B1}, v_{B2}, and v_{B3}. The twelve-pulse voltages v_{T1}, v_{T2}, and v_{T3} are connected to the three-phase power line by the coupling inductors. Current filtering at the output side of the rectifier is not required, causing the rectifier to be of the output voltage type. Actually, the current flowing to the filtering capacitor and the load contains very low ripple. The rectifier is simple and does not require any controlled switches, neither the high frequency switching. Thus, related electromagnetic interference issues, increased losses, and reduced reliability are avoided.

The basic structure proposed in [1] is extended in [2, 3] to provide 18-pulse operation and the reverse flow of energy in the recuperation mode. An extension to 24-pulse operation and detailed analysis of the rectifier are given in [4]. Although the rectifier structure is simple, it is hard to analyze it. In [5], sinusoidal approximation approach is applied to analyze six-pulse output voltage type rectifiers while they operate in the continuous conduction mode. In [6], it is shown that in the case resistive losses in the rectifier can be neglected, there is a closed-fom analytical solution that covers the rectifier behavior, having the same computation complexity as the sinusoidal approximation based solution of [5]. However, resistive losses, i.e. current dependent losses, cannot be covered by such solution.

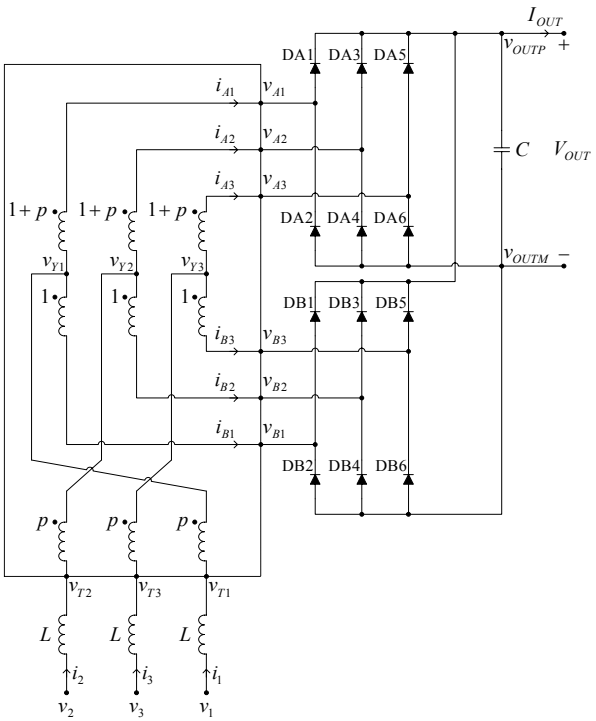

Fig. 1. *The rectifier*

Table 1. *Definitions of index functions*

k	$\uparrow(k)$	$\downarrow(k)$
1	2	3
2	3	1
3	1	2

An extension of [6] is given in [7], where a closed-form solution of the rectifier of Fig. 1, is given for the continuous conduction mode, as well as the solution based on the sinusoidal approximation. Comparison of the solutions is provided, indicating that the difference between the exact and the sinusoidal approximation based solution is lower than in the case of the six-pulse rectifier, due to the twelve-pulse operation and thus reduced harmonic content of the rectifier voltages and currents at the AC side. Again, the exact and the sinusoidal approximation based solution have the same computational complexity. Unfortunatelly, the exact solution cannot take account of resistive losses, dependent on the rectifier currents. In the area where this type of losses is relevant, sinusoidal approximation should be used, being the only choice, but justified with the good agreement with the exact solution in the case the resistive losses were absent from the circuit.

Application of the sinusoidal approximation to the analysis of the rectifier of Fig. 1 is given in this paper, and closed-form expressions for the dependence of the output voltage on the output current, as well as the output power, the power factor, and the efficiency on the output voltage are given. Experimental results obtained on the rectifier model are presented and compared to the analytical predictions.

2. SINUSOIDAL APPROXIMATION

2.1. Preliminaries

Let us assume that the rectifier is supplied by a three-phase voltage system

$$v_k = V_m \sin\left(\omega t - (k-1)\frac{2\pi}{3}\right) \tag{1}$$

for $k \in \{1, 2, 3\}$.

To simplify the notation and to reduce the number of equations that needs to be written to characterize the line-side interphase transformer (actual number of equations is nine, and cannot be reduced regardless the compact notation), let us define the index functions "next" $\uparrow(k)$ and "previous" $\downarrow(k)$, defined for $k \in \{1, 2, 3\}$. Definitions of these functions are given in Table I, being based on modular arithmetic with the base equal to 3, but shifted for 1 to meet the common indexing of phases.

After the index functions are introduced, equations that characterize the line-side interphase transformer are given by

$$i_{Ak} = \frac{1}{p+2} i_k - \frac{p}{p+2} i_{\uparrow(k)} \tag{2}$$

$$i_{Bk} = \frac{p+1}{p+2} i_k + \frac{p}{p+2} i_{\uparrow(k)} \tag{3}$$

and

$$v_{Tk} = \frac{1}{p+2} v_{Ak} + \frac{p+1}{p+2} v_{Bk} - \frac{p}{p+2}\left(v_{A\downarrow(k)} - v_{B\downarrow(k)}\right) \tag{4}$$

for $k \in \{1, 2, 3\}$. There is a total of nine such equations in the expanded form, six of them relating currents, and three of them relating voltages.

To provide twelve-pulse waveforms of v_{T1}, v_{T2}, and v_{T3} and to cancell out harmonic components at $6n \pm 1$, $n \in N$, the line-side interphase transformer turns ratio according to [1] should be set to

$$p = \frac{\sqrt{3}-1}{2} \approx 0.366 . \tag{5}$$

2.2. Normalization

In order to generalize the results, normalization of variables should be introduced. It is convenient to normalize the circuit voltages to the phase voltage amplitude

$$m = \frac{1}{V_m} v . \tag{6}$$

The time variable should be replaced by the phase angle variable

$$\varphi = \omega t . \tag{7}$$

In the case the currents are normalized according to

$$j = \frac{\omega L}{V_m} i \tag{8}$$

governing equations for the inductors reduce from

$$L\frac{di_k}{dt} = v_k - v_{Tk} \tag{9}$$

to

$$\frac{dj_k}{d\varphi} = m_k - m_{Tk} \tag{10}$$

for $k \in \{1, 2, 3\}$.

To preserve the form of Ohm's law, resistances should be normalized to

$$\rho = \frac{1}{\omega L} R . \tag{11}$$

2.3. Sinusoidal approximation

Sinusoidal approximation approach in the circuit analysis assumes negligible higher-order harmonic components of all ac waveforms. In the case of the rectifier of Fig. 1, the approximation is done around the inductors: their terminal voltages are assumed as sinusoidal, as well as their currents. Let us assume that the inductor currents are

$$j_k = J_m \sin\left(\varphi - \phi - (k-1)\frac{2\pi}{3}\right) \tag{12}$$

for $k \in \{1, 2, 3\}$, where ϕ is the phase shift of the phase currents with regard to the corresponding phase voltages. According to (2), (3), and (5), this results in the line-side interphase transformer output currents

$$j_{Ak} = \frac{\sqrt{3}-1}{\sqrt{2}} J_m \sin\left(\varphi - \phi + \frac{\pi}{12} - (k-1)\frac{2\pi}{3}\right) \tag{13}$$

and

$$j_{Bk} = \frac{\sqrt{3}-1}{\sqrt{2}} J_m \sin\left(\varphi - \phi - \frac{\pi}{12} - (k-1)\frac{2\pi}{3}\right). \tag{14}$$

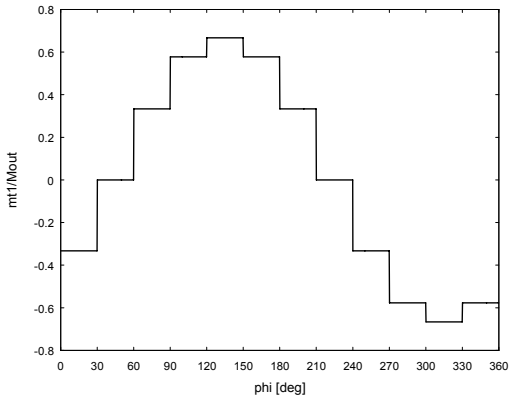

Fig. 2. *The line-side interphase transformer input voltage, v_{T1}, for $\phi = 45°$*

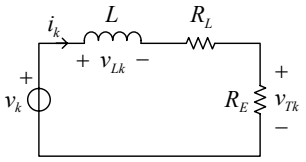

Fig. 3. *The AC-side equivalent circuit per one phase*

Generalizing the result of [5] to two three-phase diode bridges, the rectifier output current is given by

$$J_{OUT} = \frac{3}{\pi}\left(\sqrt{6}-\sqrt{2}\right)J_m \tag{15}$$

which is used in [7].

Each of the inductors has one terminal connected to a corresponding phase voltage, which is assumed as sinusoidal by (1). The inductor currents are introduced as sinusoidal by (12), which is an approximation. To complete the sinusoidal approximation, waveforms of the line-side interphase transformer input voltages v_{Tk}, $k \in \{1, 2, 3\}$, should be approximated by their sinusoidal representations. In [7], detailed analysis is performed assuming constant output voltage, and the waveforms of v_{Tk} are obtained as twelve-pulse staircase, depicted in Fig. 2 in the case of m_{T1}. It should be noted that the waveform of Fig. 2 is obtained neglecting losses in the line side interphase transformer and the diodes in the diode bridges. Approximate representation of v_{Tk} waveforms by their fundamental harmonics results in

$$m_{Tk} \approx M_{Tm1}\sin\left(\varphi - \phi - (k-1)\frac{2\pi}{3}\right) \tag{16}$$

where

$$M_{Tm} = \frac{2}{\pi}\left(\sqrt{6}-\sqrt{2}\right)M_{OUT} \tag{17}$$

which is derived in [7]. It is important to underline here that the waveforms of v_{Tk} are synchronized to the corresponding waveforms of i_{Tk}, having the same phase. Thus, the remaining nonlinear part of the rectifier that contains the line-side interphase transformer, the diode bridges, and the filtering capacitor, may be represented by three resistors of the normalized resistance

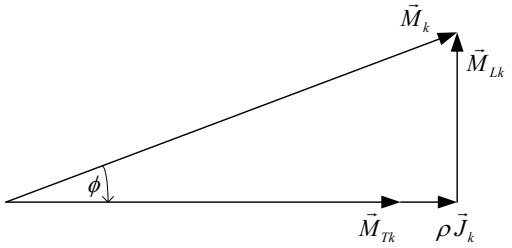

Fig. 4. *The phasor diagram*

$$\rho_E = \frac{R_E}{\omega L} = \frac{M_{Tm}}{J_m} = \frac{24}{\pi^2}\left(2-\sqrt{3}\right)\frac{M_{OUT}}{J_{OUT}} \tag{18}$$

which is the resistance emulated at the line-side interphase transformer input. In this manner, the rectifier is at the AC side represented by three identical linear equivalent circuits shown in Fig. 3 for one phase. This equivalent circuit is an essential result of sinusoidal approximation, and it provides the most important information regarding the rectifier behavior. In the equivalent circuit of Fig. 3, it is assumed that resistive losses can be modelled by a series resistance *R*. This resistance is suitable to model conduction losses in the inductors.

2.4. Solution for the rectifier operation parameters

A phasor diagram that relates normalized voltages and currents of the circuit shown in Fig. 3 is given in Fig. 4. According to the normalization (6)

$$\left|\vec{M}_k\right| = 1 \tag{19}$$

while according to (10)

$$\left|\vec{M}_{Lk}\right| = \left|\vec{J}_k\right|. \tag{20}$$

Since

$$\left|\vec{J}_k\right| = J_m \tag{21}$$

and

$$\left|\vec{M}_{Tk}\right| = M_{Tm} \tag{22}$$

normalized amplitudes of the AC quantities are related as

$$\left(M_{Tm} + \rho J_m\right)^2 + J_m^2 = 1 \tag{23}$$

which provides amplitude of the line-side interphase transformer input voltage fundamental harmonic as

$$M_{Tm} = \sqrt{1 - J_m^2} - \rho J_m. \tag{24}$$

Since

$$M_{Tm} = \frac{2}{\pi}\left(\sqrt{6}-\sqrt{2}\right)M_{OUT} \tag{25}$$

and since according to [7]

$$J_m = \frac{\pi}{3\left(\sqrt{6}-\sqrt{2}\right)}J_{OUT} \tag{26}$$

the output voltage and the output current are related as

$$\begin{aligned} M_{OUT} = \frac{\pi}{48}\Bigg(&\left(\sqrt{6}+\sqrt{2}\right)\sqrt{36-\left(2+\sqrt{3}\right)\left(\pi J_{OUT}\right)^2} - \\ &-2\pi\rho\left(2+\sqrt{3}\right)J_{OUT}\Bigg) \approx \\ \approx &\sqrt{2.3021 - 2.3554 J_{OUT}^{\ 2}} - 1.5347\rho J_{OUT}. \end{aligned} \tag{27}$$

This is the most important relation that arises from the sinusoidal approximation. All other rectifier operation parameters are derived applying this equation.

Normalized output power is given by

$$P_{OUT} = M_{OUT} J_{OUT} = \\ = \frac{3\left(\sqrt{6}-\sqrt{2}\right)}{\pi^2\left(1+\rho^2\right)} M_{OUT}\left(\sqrt{\pi^2\left(1+\rho^2\right)-16\left(2-\sqrt{3}\right)M_{OUT}^2} - \right. \\ \left. -2\left(\sqrt{6}-\sqrt{2}\right)\rho M_{OUT}\right) \tag{28}$$

and reaches its maximum for

$$\frac{dP_{OUT}}{dM_{OUT}} = 0 \tag{29}$$

at

$$M_{OUT} = \frac{\pi}{8}\left(1+\sqrt{3}\right)\sqrt{1+\rho^2-\rho\sqrt{1+\rho^2}} \tag{30}$$

of

$$P_{OUT\max} = \frac{3}{4}\left(\sqrt{1+\rho^2}-\rho\right). \tag{31}$$

The rectifier power factor, which is the same as the displacement power factor in the case the sinusoidal approximation is applied, is obtained from the phasor diagram of Fig. 4. as

$$PF = DPF = M_{Tm} + \rho J_m = \\ = \frac{2}{\pi}\left(\sqrt{6}-\sqrt{2}\right)M_{OUT} + \rho\frac{\pi}{3\left(\sqrt{6}-\sqrt{2}\right)}J_{OUT} \tag{32}$$

where M_{OUT} and J_{OUT} are related according to (27).

The analyses performed up to this point did not take into account forward voltage drop across the diodes. In cases when the input voltages are low, forward voltage drop significantly affects the results. The forward voltage drop can be incorporated in the analysis knowing that the actual output voltage is lower than predicted for twice the diode forward voltage drop. In the case of the rectifier efficiency, this technique yields

$$\eta = \frac{M_{OUT}J_{OUT}}{\left(M_{OUT}+2M_D\right)J_{OUT}+\frac{3}{2}\rho J_m^2} \tag{33}$$

where M_D is normalized value of the forward voltage drop, while J_m and J_{OUT} are related by (26).

3. EXPERIMENTAL RESULTS

To verify the analytical predictions, a low-power rectifier model is built. The model is designed to operate with the phase voltage amplitude of $V_m = 32\ \text{V}$. The coupling inductors are measured at the output current of $I_{OUT} = 4\ \text{A}$, which is the point close to the maximum of the output power. The measurement is performed by digital post processing of the voltage and current waveforms recorded across the inductors. Average inductance of the inductors is measured as $L = 17.464\ \text{mH}$, and inductances of all three inductors are within $\pm 3.5\%$ of the average value. Analyzing the rectifier losses at the same output current, the equivalent per phase resistance is determined as $R = 0.784\ \Omega$, corresponding to $\rho = 0.1429$.

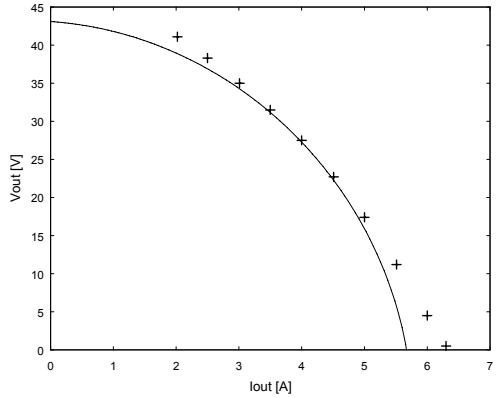

Fig. 5. *Dependence of the output voltage on the output current: crosses—experimental data; solid line—analytical prediction*

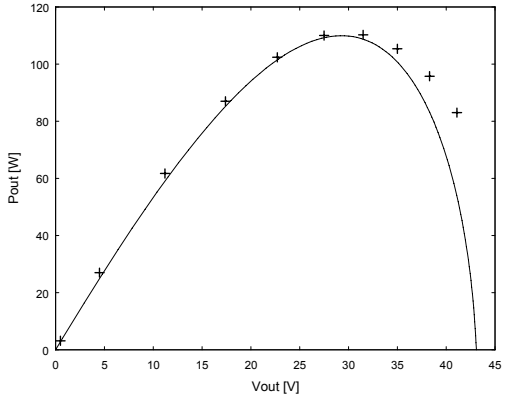

Fig. 6. *Dependence of the output power on the output voltage: crosses—experimental data; solid line—analytical prediction*

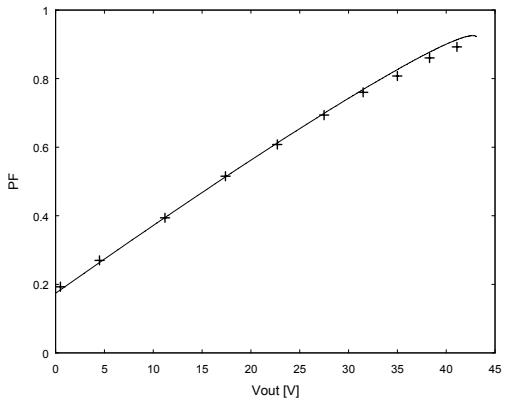

Fig. 7. *Dependence of the power factor on the output voltage: crosses—experimental data; solid line—analytical prediction*

Dependence of the output voltage on the output current is shown in Fig. 5, where crosses represent the experimental data points, while the solid line presents denormalized analytical prediction of (27). Good agreement between the results is obtained, except at the low output voltages where both the input currents and the

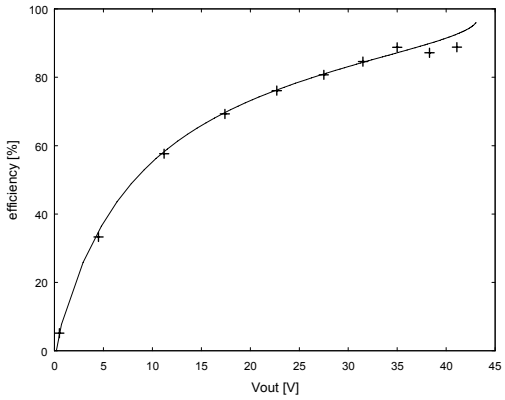

Fig. 8. *Dependence of the rectifier efficiency on the output voltage: crosses—experimental data; solid line—analytical prediction*

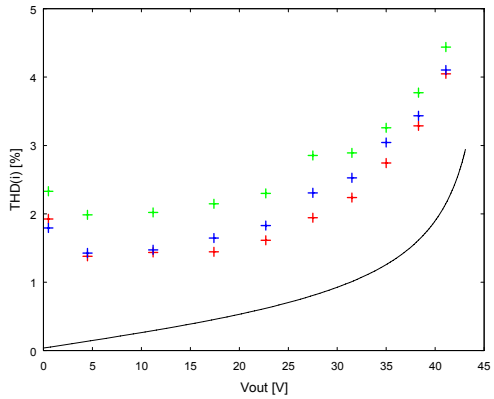

Fig. 9. *Dependence of the input current THD on the output voltage: red—phase 1; blue—phase 2; green—phase 3; black solid line—analytical prediction of [7]*

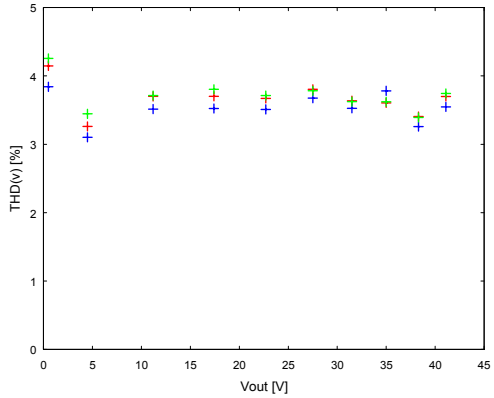

Fig. 10. *Dependence of the input voltage THD on the output voltage: red—phase 1; blue—phase 2; green—phase 3*

output current increase due to the saturation of the coupling inductors.

In Fig. 6, dependence of the output power on the output voltage is given. Again, the results are in good agreement with the analytical predictions of (28).

Dependence of the input power factor on the output voltage is presented in Fig. 7. Excellent agreement with the analytical predictions of (32) are achieved. Dependence of the rectifier efficiency on the output voltage is given Fig. 8. Experimental data are in an excellent agreement with the analytical predictions, again.

The input current THD cannot be predicted applying sinusoidal approximation, since the higher order harmonics are neglected. Prediction for the input current THD is given in [7] as a result of the exact solution of the rectifier model. However, the exact solution is available only in the case losses are negligible, i.e. $\rho = 0$. Experimentally obtained values of the input current THD are given in Fig. 9, accompanied by the curve predicted in [7] for the case $\rho = 0$. The results are in a relatively good agreement, regarding the fact that the losses are neglected, and that the input voltage THD values are as given in Fig. 10, since the available voltages were slightly distorted. Increase of the input current THD at low output voltage levels is due to the saturation of the coupling inductors.

4. CONCLUSIONS

Sinusoidal approximation approach in analysis of three-phase twelve-pulse output voltage type rectifiers is experimentally verified. To perform the analysis based on sinusoidal approximation, the rectifier input currents are assumed sinusoidal, and resulting waveforms of the rectifier voltages, primarily the input voltages of the line side interphase transformer, are obtained. The input voltages of the line side interphase transformer are approximated by their fundamental harmonics, which causes all voltages and currents at the rectifier AC side to be sinusoidal. An equivalent circuit that represents the rectifier AC side is derived. Analyzing the equivalent circuit, corresponding phasor diagram is derived, which relates quantities that yield to the equation that relates the output voltage and the output current. This relation is essential to derive all other rectifier operating parameters. The output power, the power factor, and the rectifier efficiency are determined. To verify the analytical results, a low-power rectifier model is built. Regarding the output voltage, the output power, the power factor, and the efficiency, the experimental results and the analytical predictions are in an excellent agreement. Regarding the input current THD, the agreement between the experimental results and the analytical prediction of [7] is relatively good, with some differences caused by the input voltage THD and the saturation of coupling inductors at high output currents.

5. REFERENCES

[1] M. Depenbrock, C. Niermann, "A new 12-pulse rectifier with line-side interphase transformer and nearly sinusoidal line currents," *Proceedings of the Power Electronics and Motion Control Conference*, Budapest, 1990, pp. 374-378.

[2] C. Niermann, "New rectifier circuits with low mains pollution and additional low cost inverter for energy recovery," *Proceedings of the European Power Electronics Conference*, Aachen, 1989, pp. 1131-1136.

[3] M. Depenbrock, C. Niermann, "A new 18-pulse rectifier circuit with line-side interphase transformer and nearly sinusoidal line currents," *Proceedings of the 2nd International Power Electronics Conference* (*IPEC*), Tokyo, 1990, pp. 539-546.
[4] P. Mysiak, "A 24-pulse diode rectifier with coupled three-phase reactor," *Journal of the Chinese Institute of Engineers*, Vol. 30, No. 7, pp. 1197-1212, 2007.
[5] V. Caliskan, D. J. Perreault, T. M. Jahns, and J. G. Kassakian, "Analysis of three-phase rectifiers with constant-voltage loads," *IEEE Trans. Circuits Syst. I, Fundam. Theory Appl.*, vol. 50, no. 9, pp. 1220-1226, Sep. 2003.
[6] P. Pejović, J. W. Kolar, "Exact analysis of three-phase rectifiers with constant voltage loads," *IEEE Transactions on Circuits and Systems-II: Express Briefs*, vol. 55, no. 8, pp. 743-747, Aug. 2008.
[7] P. Pejović, J. W. Kolar, "Analysis of a three-phase twelve-pulse voltage output type rectifier," submitted for review.